Acta Cryst E CRYSTALLOGRAPHIC COMMUNICATIONS

ISSN 2056-9890

Crystal structure and Hirshfeld surface analysis of 3-acetyl-11-keto-β-boswellic acid

B. Dinesh,[a] H. N. Shafiulla,[a] J. C. Shwetha,[b] A. H. Udaya Kumar,[c] N. K. Lokanath[d] and K. Anand Solomon[a]*

[a]Department of Phytochemistry, Greenspace Herbs, Brigade Twin Towers, Yeshwanthpur, Bengaluru-560022. Karnataka, India, [b]Department of Chemistry, Sri Sathya Sai University for Human Excellence, Nallakadirenahalli, 561211, India, [c]Department of Physics, Seshadripuram Institute of Technology, Kadakola industrial area, Mysore 571311, Karnataka, India, and [d]Department of Studies in Physics, University of Mysore, Mysuru 570006, Karnataka, India. *Correspondence e-mail: anand.dcb@gmail.com

Received 10 April 2026
Accepted 21 May 2026

Edited by F. F. Ferreira, Universidade Federal do ABC, Brazil

Keywords: 3-acetyl-11-keto-β-boswellic acid; hydrogen bonds; Hirshfeld surface analysis; crystal structure.

CCDC reference: 2555762

Supporting information: this article has supporting information at journals.iucr.org/e

Acetyl-11-keto-β-boswellic acid, $C_{32}H_{48}O_5$, a pentacyclic triterpenoid from *Boswellia serrata*, exhibits notable anti-inflammatory and pharmacological activities. The compound crystallizes in the orthorhombic space group $P2_12_12$ and exhibits a rigid pentacyclic framework with eleven stereogenic centers. The cyclohexane rings adopt near-ideal chair conformations with minimal steric strain. The crystal packing is governed by O—H···O hydrogen bonds, forming zigzag chains along the [100] direction and extending into a three-dimensional network and is further consolidated by van der Waals interactions. Hirshfeld surface analysis shows dominant H···H contacts (91.5%), highlighting the importance of van der Waals forces, while H···O/O···H contacts provide localized stabilization.

1. Chemical context

Acetyl-11-keto-β-boswellic acid (AKBA) is a natural compound isolated from the dried gum resin of *Boswellia Serrata*. It belongs to ursane-type pentacyclic triterpene class, containing fused cyclohexane rings. The molecule bears several oxygen-containing functional groups, including carboxylic acid, ketone, and acetyl substituents (Park *et al.*, 2002), which contribute to intermolecular interactions within the crystal. The cardioprotective activity of these compounds has been recorded (Teng *et al.*, 2024). AKBA exhibits inhibitory effects on cultured human umbilical vascular endothelial cells (Shen *et al.*, 2015), and also exhibits anti-proliferative (Li *et al.*, 2022), and anti-dermatitis (Tsai *et al.*, 2022) activity. It functions as a selective inhibitor of 5-lipoxygenase, a key enzyme in leukotriene biosynthesis, with demonstrated anti-inflammatory and anti-arthritic activity (Sailer *et al.*, 1996). The molecule's lipophilic nature, inherent to its steroid-like scaffold, presents formulation challenges but also enables membrane permeability and interaction with hydrophobic enzyme active sites (Lindner *et al.*, 2026).

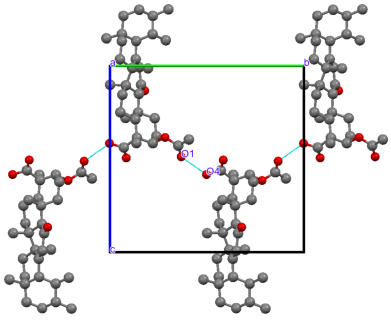

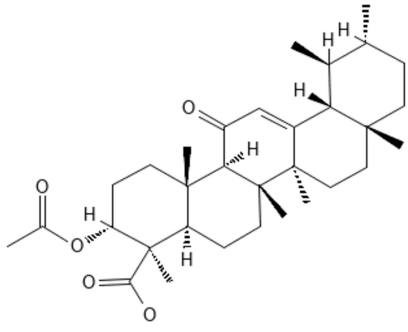

2. Structural commentary

The title molecule (Fig. 1) crystallizes in orthorhombic system, space group $P2_12_12$, with four molecules in the unit cell (Z = 4). AKBA possesses eleven stereogenic centres – C3, C4, C5, C8, C9, C17, C18, C20 in the *R* configuration and C10, C14, C19 in the *S* configuration. The acetoxy group is at the α position (Ito *et al.*, 2025*a*). This forces a planar arrangement of the six atoms O3/C9/C11–C14, with deviations from the least-square plane being less than 0.036 Å. The five six-membered rings are fused in such a manner that the C—C bonds occupy equatorial positions, except for the C18—C19 bond, which is in an axial position with respect to the C13–C18 ring. As a consequence, all cyclohexane rings form a sheet-like structure, apart from the C17–C22 ring, which is oriented roughly orthogonal to this plane [C13—C18—C17—C22 = 174.78 (4)°]. A puckering analysis of conformational characteristics of the fused six-membered rings according to the Cremer-Pople approach was quantitatively evaluated and revealed that the crystal structure exhibits mainly distorted chair-like conformational forms.

For Ring (1) (C1–C5/C10), the puckering parameters are Q = 0.541 (4) Å, θ = 5.9 (4)° and φ = 320 (4)° indicating an almost ideal chair conformation. The very small θ value together with the dominant $Q(3)$ contribution [0.538 (4) Å] confirms that the ring closely resembles a classical cyclohexane chair geometry. This assignment is further supported by the alternating torsion angles ranging from −55.2 (4) to 55.1 (4)° and by the Evans–Boeyens conformational analysis, which describes the ring as very similar to a C-form.

Ring (2) (C5–C10) also adopts a chair conformation with puckering parameters Q = 0.547 (4) Å, θ = 13.4 (4)° and φ = 25.3 (16)°. Although the θ value is slightly larger than that observed for Ring (1), the dominant $Q(3)$ term [0.532 (4) Å] clearly establishes a chair-type geometry with minor distortion. The observed torsion angles, varying between −63.3 (4) and 57.9 (4)°, are consistent with a puckered cyclohexane framework.

In contrast, Ring (3) (C8/C9/C11–C14) exhibits a significantly distorted conformation arising from the presence of sp^2-hybridized atoms within the ring skeleton. The Cremer–Pople parameters [Q = 0.563 (4) Å, θ = 54.4 (4)°, φ = 6.5 (5)°] indicate a conformation intermediate between a half-chair and twist-boat geometry. The comparatively large $Q(2)$ value [0.458 (4) Å] demonstrates a substantial deviation from an ideal chair form, while the reduced average torsion angle of approximately 40.7° further supports the presence of conformational distortion induced by partial unsaturation.

Ring (4) (C13–C18) adopts an inverted chair conformation, as evidenced by the puckering parameters Q = 0.517 (4) Å, θ = 160.4 (4)°, and φ = 41.8 (14)°. The θ value approaching 180° is characteristic of an inverted-chair geometry, while the dominant negative $Q(3)$ component [−0.487 (4) Å] further substantiates this assignment. The alternating torsion angles observed within the ring are typical of a puckered six-membered ring adopting a chair-like arrangement with slight distortion due to substitution effects.

Similarly, Ring (5) (C17–C22) displays a near-ideal inverted-chair conformation with puckering parameters Q = 0.528 (5) Å, θ = 174.0 (5)° and φ = 27 (5)°. The negligible $Q(2)$ contribution together with the dominant negative $Q(3)$ value [−0.525 (5) Å] confirms the highly stable chair geometry. The Evans–Boeyens analysis also classifies this ring as being very close to a C-form conformation.

The six-membered ring is composed of sp^3-hybridized atoms, with normal bond lengths between carbon atoms (1.5416 Å) and bond angles close to tetrahedral, suggesting a strain-free saturated ring system. The presence of alternating torsion angles, approximately ±50°, together with small deviations from planarity, is consistent with a puckered ring conformation

3. Supramolecular features and Hirshfeld surface analysis

In the extended structure of AKBA, the molecules are linked by O—H···O hydrogen bonds (Table 1) from the carboxylic

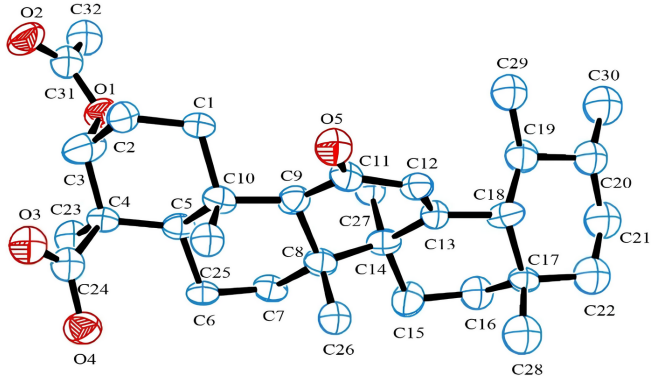

Figure 1
Acetyl-11-keto-β-boswellic acid (AKBA) showing the atomic numbering scheme. Displacement ellipsoids are drawn at the 30% probability level, and hydrogen atoms are omitted for clarity.

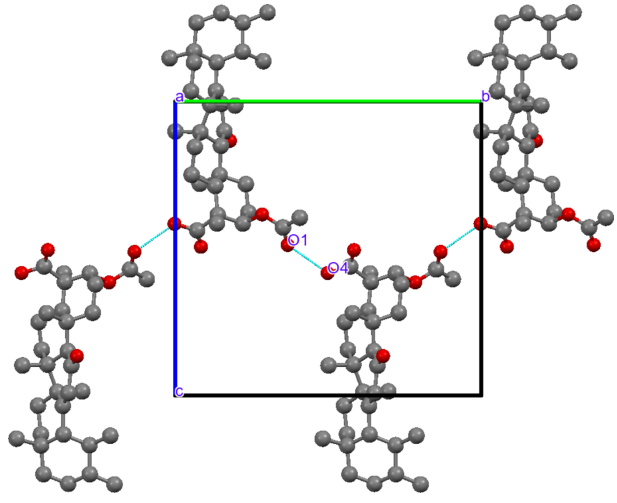

Figure 2
Crystal packing of acetyl-11-keto-β-boswellic acid (AKBA) viewed along the *c* axis, illustrating the molecular arrangement within the unit cell. Intermolecular interactions and packing orientation are highlighted, and the unit-cell boundaries are shown.

Table 1
Hydrogen-bond geometry (Å, °).

D—H···A	D—H	H···A	D···A	D—H···A
O4—H4···O1^{i}	0.82	1.91	2.695 (4)	161
C1—H1A···O5	0.97	2.39	3.023 (5)	122
C25—H25C···O5	0.96	2.38	3.058 (5)	127
C30—H30B···O1^{ii}	0.96	2.60	3.468 (6)	151
C32—H32C···O3^{iii}	0.96	2.52	3.445 (6)	162

Symmetry codes: (i) $-x+\frac{3}{2}, y-\frac{1}{2}, -z+3$; (ii) $x, y, z-1$; (iii) $x-\frac{1}{2}, -y+\frac{1}{2}, -z+3$.

acid OH group to the carbonyl oxygen atom, forming a *C*4 zigzag chain propagating along the [100] direction (Fig. 2). The hydrocarbon framework of the molecule forms hydrophobic regions, while the oxygenated functional groups participate in hydrogen bonding, leading to an organized packing arrangement within the orthorhombic structure.

The Hirshfeld surface mapped over d_{norm} for AKBA reveals localized red regions corresponding to short intermolecular contacts involving oxygen-containing functional groups. These red spots are associated mainly with close H···O/O···H interactions involving the acetyl, keto and carboxylic oxygen atoms, indicating contacts shorter than the sum of the corresponding van der Waals radii. White areas correspond to contacts close to van der Waals separations, whereas blue regions represent distances longer than the van der Waals radii and therefore weaker intermolecular contacts.

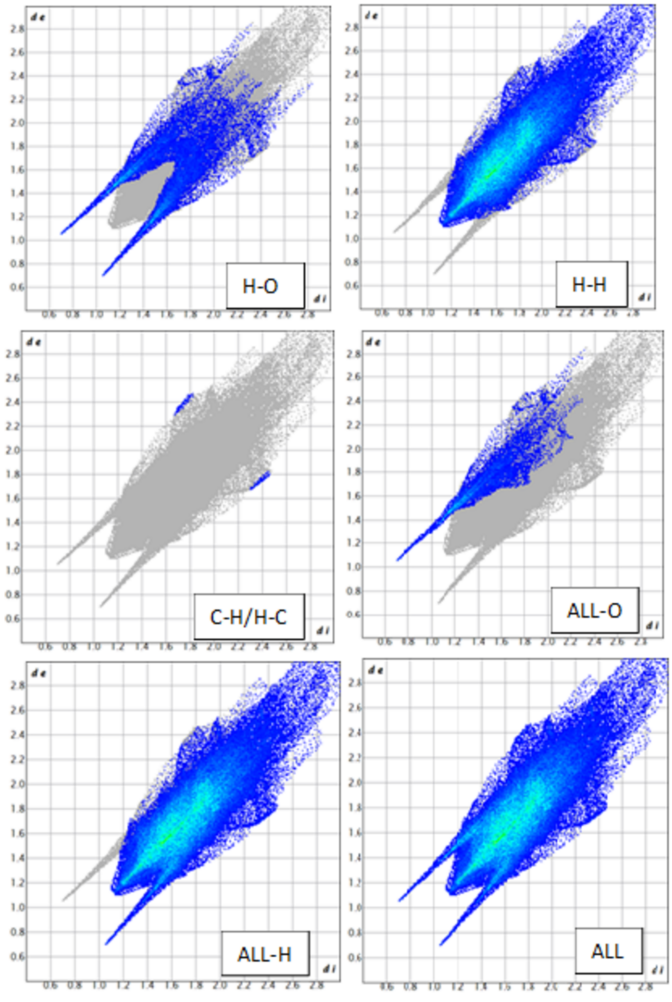

Figure 3
Hirshfeld surface fingerprint plots for acetyl-11-keto-β-boswellic acid (AKBA) showing the contributions of different intermolecular contacts: H···O/O···H, H···H, C···H/H···C, and all contacts (ALL and ALL–H). The blue regions represent the specific interactions within the molecule, while the grey areas correspond to the overall fingerprint plots. These plots highlight the dominant role of H···H and H···O interactions in consolidating the crystal packing.

The Hirshfeld surface area was calculated as 509.74 Å, with a surface volume of 755.63 Å. The globularity value of 0.787 indicates a compact but slightly elongated molecular envelope consistent with the rigid pentacyclic triterpenoid framework, whereas the asphericity value of 0.187 reflects moderate anisotropy arising from the extended substituent groups. Two-dimensional fingerprint plots show that H···H contacts dominate the crystal packing, contributing 91.5% of the total Hirshfeld surface. The broad central distribution in the H···H fingerprint plot reflects extensive hydrocarbon–hydrocarbon interactions arising from the large pentacyclic triterpenoid framework, confirming that van der Waals interactions are the principal consolidating force in the crystal. H···O/O···H contacts contribute 8.3% of the Hirshfeld surface and appear as distinct sharp spikes in the fingerprint plot. These spikes correspond to short intermolecular contacts involving oxygen acceptor atoms and indicate weak C—H···O interactions that provide localized consolidation around the polar functional groups. The reciprocal O···H/H···O contribution amounts to 17.6% when reciprocal contacts are considered, reflecting the combined donor–acceptor interaction environment surrounding the oxygen atoms. C···H/H···C contacts contribute only 0.2% of the surface and are represented by small isolated wing-like regions, indicating that weak hydrophobic carbon–hydrogen contacts make only a minor contribution to crystal packing. C···O/O···C interactions are negligible (0.1–0.2%), showing that direct carbonyl–carbon contacts are not significant in the present crystal structure (Fig. 3). The Hirshfeld surface mapped over d_{norm} displays several small bright-red spots, corresponding to weak and longer range

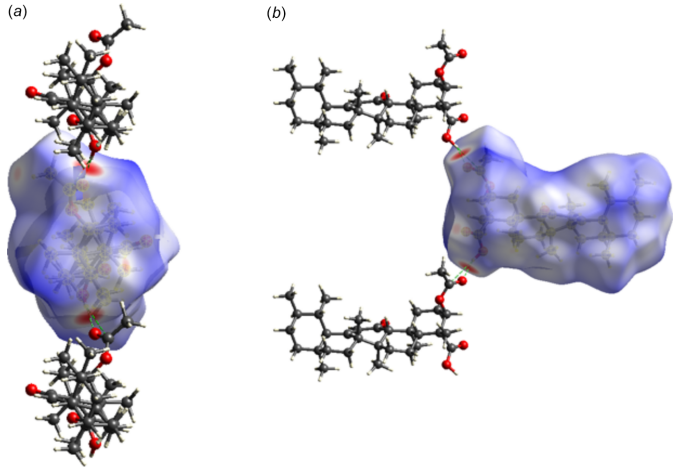

Figure 4
Hirshfeld surfaces mapped over d_{norm}: (*a*) front view and (*b*) side view showing short intermolecular contacts as red regions.

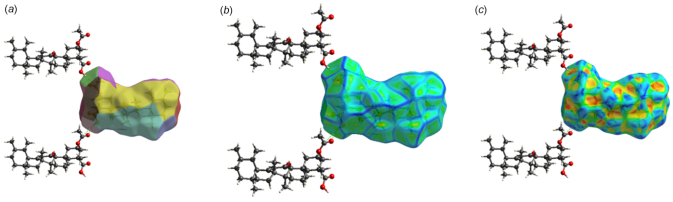

Figure 5
Hirshfeld surfaces mapped over (*a*) fragment patch, (*b*) curvedness and (*c*) shape-index, showing neighbouring molecular fragments and local surface features associated with the intermolecular packing.

interactions that contribute to the consolidation of the packing (Fig. 4). The fragment patch highlights key neighbouring molecular interactions contributing to the crystal packing. The curvedness map indicates predominantly flat regions, suggesting the absence of significant π–π stacking interactions. The shape-index surface shows complementary patterns, confirming localized intermolecular contacts such as hydrogen bonding (Fig. 5).

4. Database survey

A search of the Cambridge Structural Database (CSD, version 6.00 update of May 2025; Groom *et al.*, 2016) for compounds containing the boswellic acid skeleton shows that only a limited number of crystal structures of boswellic acid derivatives have been reported. These include β-boswellic acid, acetyl-β-boswellic acid, and 11-keto-β-boswellic acid derivatives (Majeed *et al.*, 2024; Ito *et al.*, 2025*b*). These compounds share the same pentacyclic triterpenoid framework composed of fused cyclohexane rings, adopting stable chair or slightly distorted chair conformations. In all the structures, the stereochemistry at the ring junctions remains conserved, confirming that chemical modifications at peripheral positions do not significantly alter the rigid triterpenoid backbone. Comparison with previously reported boswellic acid structures indicates that the overall structure conforms with those with other derivatives of the boswellic acid family (Fig. 6). However, substitution at the C3 and C11 positions significantly influences the intermolecular interactions and crystal packing (Al-Harrasi *et al.*, 2018). In β-boswellic acid, the hydroxyl group at C3 can participate as a hydrogen-bond donor, frequently forming intermolecular O—H···O hydrogen bonds that contribute to crystal cohesion. In addition, the compound contains an acetyl group at C3, which replaces the hydroxyl donor with an ester carbonyl acceptor, thereby reducing classical hydrogen-bonding capability (Khaafi & Javadi, 2023)

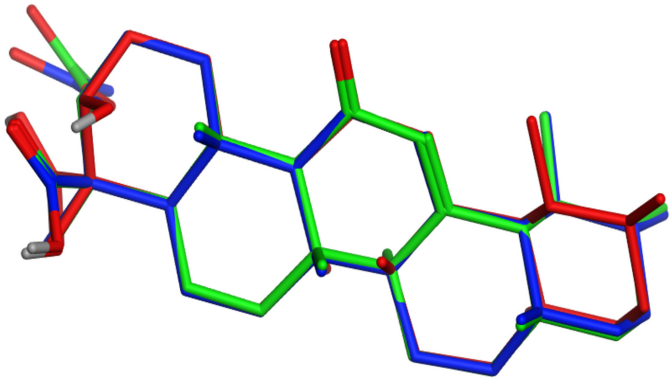

Figure 6
Superimposed molecular structures of boswellic acid derivatives showing conformational differences: acetyl β-boswellic acid (blue), 11-keto-β-boswellic acid (red) and acetyl-11-keto-β-boswellic acid (green).

Table 2
Experimental details.

Crystal data	
Chemical formula	$C_{32}H_{48}O_5$
M_r	512.70
Crystal system, space group	Orthorhombic, $P2_12_12$
Temperature (K)	293
a, b, c (Å)	11.8995 (8), 16.3460 (9), 15.7065 (9)
V (Å^3)	3055.0 (3)
Z	4
Radiation type	Mo $K\alpha$
μ (mm^{-1})	0.07
Crystal size (mm)	0.26 × 0.24 × 0.22
Data collection	
Diffractometer	Rigaku **model?**
Absorption correction	Multi-scan (*CrysAlis PRO*; Rigaku OD, 2024)
T_{min}, T_{max}	0.981, 0.984
No. of measured, independent and observed [$I > 2\sigma(I)$] reflections	21419, 6775, 3256
R_{int}	0.071
(sin $\theta/\lambda)_{max}$ (Å^{-1})	0.662
Refinement	
$R[F^2 > 2\sigma(F^2)]$, $wR(F^2)$, S	0.058, 0.155, 0.95
No. of reflections	6775
No. of parameters	344
H-atom treatment	H-atom parameters constrained
$\Delta\rho_{max}$, $\Delta\rho_{min}$ (e Å^{-3})	0.17, −0.16
Absolute structure	Flack x determined using 990 quotients $[(I^+)-(I^-)]/[(I^+)+(I^-)]$ (Parsons *et al.*, 2013)
Absolute structure parameter	0.6 (10)

Computer programs: *CrysAlis PRO* (Rigaku OD, 2024), *SHELXS* (Sheldrick, 2008), *SHELXL2018/3* (Sheldrick, 2015) and *OLEX2* (Dolomanov *et al.*, 2009).

5. Synthesis and crystallization

Fresh frankincense resin lumps of 6 g were ground to a fine, uniform powder with a mortar and pestle. Primarily, 100 mg of powdered resin was transferred into a 2 mL reaction tube and 1 mL of extraction solvent (methanol: 1% aqueous formic acid, 65:35 *v*/*v*) was added. To promote efficient release of triterpenes, the suspension was sonicated at 298 K for 10 minutes and then centrifuged at 14,000 r.p.m. for 5 minutes; the clear supernatant was decanted and reserved. The pooled AKBA-rich supernatent was subjected to flash chromatography on silica (230–400 mesh) using *n*-hexane (solvent A) and ethyl acetate (solvent B) with a gentle gradient (flow $\simeq$ 1 mL min^{-1}), guided by TLC. Fractions eluting at ∼40–50% EtOAc were concentrated under reduced pressure at low bath temperature. Residual non-polar impurities were removed by washing the concentrate with cold *n*-hexane; the remaining

polar residue was dissolved in minimum hot acetonitrile and allowed to cool slowly to room temperature (Gupta *et al.*, 2021; Lauss *et al.*, 2024). The resulting pale-white crystals were collected by filtration and dried under vacuum. Equimolar quantities (1:1 stoichiometric ratio) of AKBA crystals and cinnamic acid were dissolved in hot ethanol to obtain a clear homogeneous solution. The resulting solution was then allowed to cool slowly and allowed slow evaporation to obtain crystals suitable for SXRD analysis.

6. Refinement

Crystal data, data collection and structure refinement details are summarized in Table 2. All hydrogen atoms were placed at idealized positions C—H = 0.96–0.98 Å) and refined using a riding model with U_{iso}(H) = 1.2–1.5U_{eq}(C). The assignment of the absolute configuration is based on IUPAC nomenclature.

Acknowledgements

The author(*s*) express their sincere gratitude to Ms Tahira H. S., Chief of Research and Development at Green Space Herbs, for her valuable guidance, insightful discussions, and continuous support throughout the course of this work. The author(*s*) also appreciate the resources and facilities provided by Green Space Herbs.

References

Al-Harrasi, A., Rehman, N. U., Khan, A. L., Al-Broumi, M., Al-Amri, I., Hussain, J., Hussain, H. & Csuk, R. (2018). *PLoS One* **13**, e0198666.
Dolomanov, O. V., Bourhis, L. J., Gildea, R. J., Howard, J. A. K. & Puschmann, H. (2009). *J. Appl. Cryst.* **42**, 339–341.
Groom, C. R., Bruno, I. J., Lightfoot, M. P. & Ward, S. C. (2016). *Acta Cryst.* B**72**, 171–179.
Gupta, M., Kumar, S., Kumar, R., Kumar, A., Verma, R., Darokar, M. P., Rout, P. & Pal, A. (2021). *Biomed. Pharmacother.* **144**, 112302.
Ito, M., Misao, K., Suzuki, H. & Noguchi, S. (2025*a*). *Chem. Pharm. Bull.* **73**, 314–317.
Ito, M., Misao, K., Suzuki, H. & Noguchi, S. (2025*b*). *Chem. Pharm. Bull. (Tokyo)* **73**, 314–317.
Khaafi, F. & Javadi, B. (2023). *Mini Rev. Med. Chem.* **23**, 1912–1925.
Lauss, J., Kappacher, C., Isser, O., Huck, C. W. & Rainer, M. (2024). *Spectrochim. Acta A Mol. Biomol. Spectrosc.* **316**, 124384.
Li, C., He, Q., Xu, Y., Lou, H. & Fan, P. (2022). *ACS Omega* **7**, 9853–9866.
Lindner, S., Keim, S., Haddadzadegan, S., Fernandez Romero, O., Zöller, K., Stern, G., Cesi, I., Kafedjiiski, K. & Bernkop–Schnürch, A. (2026). *Adv. Healthc. Mater.* **15**, e03721.
Majeed, A., Majeed, S., Satish, G., Manjunatha, R., Rabbani, S. N., Patil, N. V. P. & Mundkur, L. (2024). *Front. Pharmacol.* **15**, 1428440.
Park, Y. S., Lee, J. H., Bondar, J., Harwalkar, J. A., Safayhi, H. & Golubic, M. (2002). *Planta Med.* **68**, 397–401.
Parsons, S., Flack, H. D. & Wagner, T. (2013). *Acta Cryst.* B**69**, 249–259.
Rigaku OD (2024). *CrysAlis PRO*. Rigaku Oxford Diffraction, Yarnton, England.
Sailer, E. R., Subramanian, L. R., Rall, B., Hoernlein, R. F., Ammon, H. P. & Safayhi, H. (1996). *Br. J. Pharmacol.* **117**, 615–618.
Sheldrick, G. M. (2008). *Acta Cryst.* A**64**, 112–122.
Sheldrick, G. M. (2015). *Acta Cryst.* C**71**, 3–8.
Shen, S., Xu, X., Liu, Z., Liu, J. & Hu, L. (2015). *Bioorg. Med. Chem.* **23**, 1982–1993.
Teng, W., Zhou, Z., Cao, J. & Guo, Q. (2024). *Foods* **13**, 2226.
Tsai, Y.-C., Chang, H.-H., Chou, S.-C., Chu, T. W., Hsu, Y.-J., Hsiao, C.-Y., Lo, Y.-H., Wu, N.-L., Chang, D.-C. & Hung, C.-F. (2022). *Int. J. Mol. Sci.* **23**, 9863.

supporting information

Acta Cryst. (2026). E**82**, 738-742 [https://doi.org/10.1107/S2056989026005360]

Crystal structure and Hirshfeld surface analysis of 3-acetyl-11-keto-*β*-boswellic acid

B. Dinesh, H. N. Shafiulla, J. C. Shwetha, A. H. Udaya Kumar, N. K. Lokanath and K. Anand Solomon

Computing details

3-Acetyl-11-keto-*β*-boswellic acid

Crystal data

$C_{32}H_{48}O_5$
M_r = 512.70
Orthorhombic, $P2_12_12$
a = 11.8995 (8) Å
b = 16.3460 (9) Å
c = 15.7065 (9) Å
V = 3055.0 (3) Å^3
Z = 4
$F(000)$ = 1120
D_x = 1.115 Mg m^{-3}
Mo $K\alpha$ radiation, λ = 0.71073 Å
Cell parameters from 6775 reflections
θ = 1.8–28.1°
μ = 0.07 mm^{-1}
T = 293 K
Rock, white
0.26 × 0.24 × 0.22 mm

Data collection

Rigaku **model?**
diffractometer
Multi–scan
Absorption correction: multi-scan (CrysAlis PRO; Rigaku OD, 2024)
T_{min} = 0.981, T_{max} = 0.984
21419 measured reflections
6775 independent reflections
3256 reflections with $I > 2\sigma(I)$
R_{int} = 0.071
θ_{max} = 28.1°, θ_{min} = 1.8°
h = −15→13
k = −21→20
l = −16→20

Refinement

Refinement on F^2
Least-squares matrix: full
$R[F^2 > 2\sigma(F^2)]$ = 0.058
$wR(F^2)$ = 0.155
S = 0.95
6775 reflections
344 parameters
0 restraints
Hydrogen site location: inferred from neighbouring sites
H-atom parameters constrained
$w = 1/[\sigma^2(F_o^2) + (0.0631P)^2]$ where $P = (F_o^2 + 2F_c^2)/3$
$(\Delta/\sigma)_{max}$ = 0.004
$\Delta\rho_{max}$ = 0.17 e Å^{-3}
$\Delta\rho_{min}$ = −0.16 e Å^{-3}
Extinction correction: SHELXL-2018/3 (Sheldrick 2015), $Fc^*=kFc[1+0.001xFc^2\lambda^3/\sin(2\theta)]^{-1/4}$
Extinction coefficient: 0.0054 (14)
Absolute structure: Flack x determined using 990 quotients $[(I^+)-(I^-)]/[(I^+)+(I^-)]$ (Parsons *et al.*, 2013)
Absolute structure parameter: 0.6 (10)

Special details

Geometry. All esds (except the esd in the dihedral angle between two l.s. planes) are estimated using the full covariance matrix. The cell esds are taken into account individually in the estimation of esds in distances, angles and torsion angles; correlations between esds in cell parameters are only used when they are defined by crystal symmetry. An approximate (isotropic) treatment of cell esds is used for estimating esds involving l.s. planes.

Fractional atomic coordinates and isotropic or equivalent isotropic displacement parameters (Å²)

	x	*y*	*z*	U_{iso}*/U_{eq}
C18	0.8263 (3)	0.1344 (2)	0.8671 (2)	0.0647 (10)
H18	0.904794	0.127092	0.849952	0.078*
O2	0.6711 (2)	0.28353 (14)	1.38435 (16)	0.0754 (8)
C9	0.8163 (3)	0.14879 (19)	1.1508 (2)	0.0547 (9)
H9	0.774299	0.199366	1.140404	0.066*
C5	0.7083 (3)	0.1303 (2)	1.2877 (2)	0.0584 (10)
H5	0.663179	0.175629	1.265316	0.070*
C13	0.8257 (3)	0.1324 (2)	0.9645 (2)	0.0581 (10)
C10	0.8270 (3)	0.14465 (19)	1.2504 (2)	0.0565 (9)
C11	0.9241 (3)	0.1600 (2)	1.1012 (3)	0.0635 (10)
C7	0.6369 (3)	0.0635 (2)	1.1551 (2)	0.0654 (10)
H7A	0.584322	0.107890	1.145585	0.079*
H7B	0.603323	0.013902	1.132752	0.079*
C3	0.7493 (4)	0.2204 (2)	1.4153 (3)	0.0691 (11)
H3	0.753162	0.222089	1.477613	0.083*
C6	0.6541 (3)	0.0534 (2)	1.2496 (2)	0.0678 (11)
H6A	0.702046	0.006512	1.260158	0.081*
H6B	0.582292	0.043524	1.276925	0.081*
C12	0.9183 (3)	0.15086 (19)	1.0080 (3)	0.0621 (10)
H12	0.984190	0.158588	0.977235	0.075*
C4	0.6985 (3)	0.1387 (2)	1.3861 (2)	0.0656 (11)
O4	0.7212 (3)	−0.00278 (16)	1.41652 (18)	0.1025 (11)
H4	0.735364	−0.035366	1.454747	0.154*
C1	0.8679 (3)	0.2302 (2)	1.2813 (3)	0.0677 (11)
H1A	0.944279	0.238967	1.261724	0.081*
H1B	0.820861	0.272144	1.256037	0.081*
C16	0.6425 (3)	0.0608 (3)	0.8678 (3)	0.0859 (13)
H16A	0.605178	0.111622	0.853010	0.103*
H16B	0.599911	0.016317	0.842725	0.103*
O5	1.0147 (2)	0.17837 (18)	1.13377 (17)	0.0879 (9)
C8	0.7460 (3)	0.08150 (18)	1.1051 (2)	0.0555 (9)
C2	0.8643 (4)	0.2384 (2)	1.3777 (3)	0.0761 (12)
H2A	0.918751	0.201162	1.402420	0.091*
H2B	0.886217	0.293623	1.393160	0.091*
C15	0.6423 (4)	0.0511 (2)	0.9652 (3)	0.0806 (13)
H15A	0.667898	−0.003545	0.979415	0.097*
H15B	0.565750	0.056592	0.985766	0.097*
C19	0.7893 (3)	0.2195 (2)	0.8309 (2)	0.0696 (11)
H19	0.712948	0.230256	0.851441	0.083*

C14	0.7174 (3)	0.1142 (2)	1.0119 (2)	0.0595 (9)
C17	0.7617 (4)	0.0611 (2)	0.8298 (3)	0.0804 (12)
O3	0.8236 (3)	0.08341 (17)	1.4943 (2)	0.0934 (10)
C27	0.6491 (3)	0.1955 (2)	1.0140 (3)	0.0726 (11)
H27A	0.699187	0.240449	1.024465	0.109*
H27B	0.594032	0.192863	1.058563	0.109*
H27C	0.612170	0.203254	0.960296	0.109*
O1	0.7217 (3)	0.36657 (16)	1.4882 (2)	0.1078 (12)
C23	0.7574 (4)	0.0711 (2)	1.4386 (3)	0.0768 (12)
C26	0.8150 (3)	0.0004 (2)	1.1019 (3)	0.0733 (11)
H26A	0.889530	0.011747	1.081631	0.110*
H26B	0.778888	−0.037538	1.064171	0.110*
H26C	0.819116	−0.022762	1.157962	0.110*
C24	0.5746 (4)	0.1356 (2)	1.4149 (3)	0.0872 (13)
H24A	0.531034	0.172939	1.381207	0.131*
H24B	0.569626	0.150849	1.473828	0.131*
H24C	0.546079	0.081116	1.407668	0.131*
C25	0.9125 (3)	0.0795 (2)	1.2798 (3)	0.0734 (11)
H25A	0.880435	0.025969	1.272972	0.110*
H25B	0.930777	0.088241	1.338604	0.110*
H25C	0.979502	0.083631	1.245995	0.110*
C20	0.7854 (4)	0.2204 (3)	0.7323 (3)	0.0883 (13)
H20	0.862199	0.211959	0.711537	0.106*
C22	0.7544 (5)	0.0691 (3)	0.7322 (3)	0.1049 (16)
H22A	0.828239	0.058615	0.708462	0.126*
H22B	0.704266	0.026918	0.710992	0.126*
C31	0.6617 (4)	0.3518 (2)	1.4287 (3)	0.0771 (12)
C32	0.5735 (4)	0.4064 (2)	1.3955 (3)	0.0976 (14)
H32A	0.563288	0.396468	1.335755	0.146*
H32B	0.595476	0.462339	1.404077	0.146*
H32C	0.504313	0.396088	1.425005	0.146*
C29	0.8637 (4)	0.2875 (3)	0.8631 (3)	0.0955 (14)
H29A	0.860074	0.289520	0.924169	0.143*
H29B	0.838636	0.338766	0.840076	0.143*
H29C	0.939856	0.277619	0.845714	0.143*
C21	0.7141 (5)	0.1502 (4)	0.6997 (3)	0.1055 (16)
H21A	0.636805	0.158426	0.717432	0.127*
H21B	0.715825	0.149903	0.637999	0.127*
C28	0.8231 (5)	−0.0187 (3)	0.8530 (3)	0.1089 (16)
H28A	0.893397	−0.021101	0.823039	0.163*
H28B	0.777492	−0.064642	0.837109	0.163*
H28C	0.836816	−0.020016	0.913169	0.163*
C30	0.7443 (5)	0.3010 (3)	0.6975 (3)	0.1197 (18)
H30A	0.671966	0.313323	0.721263	0.179*
H30B	0.738440	0.297557	0.636666	0.179*
H30C	0.796512	0.343426	0.712480	0.179*

Atomic displacement parameters (Å²)

	U^{11}	U^{22}	U^{33}	U^{12}	U^{13}	U^{23}
C18	0.055 (2)	0.065 (2)	0.074 (3)	−0.0002 (19)	0.010 (2)	−0.0078 (19)
O2	0.095 (2)	0.0501 (14)	0.0807 (17)	0.0167 (14)	−0.0065 (15)	−0.0069 (13)
C9	0.047 (2)	0.0423 (18)	0.075 (3)	−0.0010 (16)	−0.0059 (19)	0.0048 (17)
C5	0.056 (2)	0.0433 (19)	0.076 (3)	−0.0002 (16)	−0.004 (2)	0.0051 (17)
C13	0.048 (2)	0.0461 (19)	0.081 (3)	0.0030 (17)	0.003 (2)	−0.0013 (18)
C10	0.050 (2)	0.0402 (18)	0.080 (3)	0.0024 (17)	−0.0068 (19)	0.0021 (17)
C11	0.044 (2)	0.057 (2)	0.090 (3)	−0.0059 (18)	−0.004 (2)	0.008 (2)
C7	0.055 (2)	0.060 (2)	0.081 (3)	−0.0107 (19)	0.000 (2)	0.0023 (19)
C3	0.088 (3)	0.050 (2)	0.069 (2)	0.010 (2)	−0.010 (2)	0.0003 (18)
C6	0.067 (3)	0.056 (2)	0.081 (3)	−0.009 (2)	0.003 (2)	0.0057 (19)
C12	0.044 (2)	0.062 (2)	0.080 (3)	−0.0035 (18)	0.005 (2)	0.004 (2)
C4	0.075 (3)	0.047 (2)	0.075 (3)	0.0000 (18)	−0.004 (2)	−0.0002 (19)
O4	0.160 (3)	0.0521 (16)	0.095 (2)	−0.0083 (18)	−0.029 (2)	0.0153 (15)
C1	0.062 (2)	0.055 (2)	0.087 (3)	−0.0079 (19)	−0.011 (2)	−0.002 (2)
C16	0.069 (3)	0.105 (3)	0.084 (3)	−0.026 (3)	−0.002 (2)	−0.018 (2)
O5	0.0552 (18)	0.111 (2)	0.097 (2)	−0.0199 (15)	−0.0107 (16)	0.0098 (17)
C8	0.043 (2)	0.0477 (18)	0.076 (2)	−0.0030 (16)	−0.0002 (19)	0.0029 (18)
C2	0.088 (3)	0.049 (2)	0.091 (3)	0.000 (2)	−0.027 (3)	−0.008 (2)
C15	0.061 (3)	0.097 (3)	0.084 (3)	−0.024 (2)	−0.001 (2)	−0.006 (2)
C19	0.061 (3)	0.077 (3)	0.071 (3)	0.004 (2)	0.005 (2)	0.003 (2)
C14	0.044 (2)	0.060 (2)	0.074 (2)	−0.0042 (17)	−0.0025 (19)	0.0024 (19)
C17	0.078 (3)	0.082 (3)	0.082 (3)	−0.013 (3)	0.011 (3)	−0.019 (2)
O3	0.120 (3)	0.0680 (18)	0.092 (2)	0.0050 (17)	−0.027 (2)	0.0057 (16)
C27	0.053 (2)	0.085 (3)	0.080 (3)	0.017 (2)	0.004 (2)	0.009 (2)
O1	0.176 (3)	0.0553 (16)	0.092 (2)	0.0202 (19)	−0.026 (2)	−0.0187 (16)
C23	0.103 (4)	0.046 (2)	0.081 (3)	0.005 (2)	0.001 (3)	0.005 (2)
C26	0.070 (3)	0.051 (2)	0.099 (3)	−0.0016 (18)	−0.003 (2)	−0.001 (2)
C24	0.089 (3)	0.076 (3)	0.097 (3)	0.001 (2)	0.022 (3)	−0.002 (2)
C25	0.067 (3)	0.063 (2)	0.090 (3)	0.012 (2)	−0.008 (2)	0.008 (2)
C20	0.087 (3)	0.101 (3)	0.076 (3)	−0.004 (3)	0.015 (3)	−0.005 (3)
C22	0.108 (4)	0.113 (4)	0.094 (4)	−0.029 (4)	0.014 (3)	−0.035 (3)
C31	0.107 (4)	0.049 (2)	0.076 (3)	0.001 (2)	0.006 (3)	−0.002 (2)
C32	0.109 (4)	0.062 (2)	0.122 (4)	0.024 (3)	0.010 (3)	0.006 (3)
C29	0.108 (4)	0.075 (3)	0.103 (3)	−0.009 (3)	−0.017 (3)	0.010 (2)
C21	0.114 (4)	0.129 (4)	0.074 (3)	−0.011 (4)	0.003 (3)	−0.006 (3)
C28	0.118 (4)	0.068 (3)	0.141 (4)	−0.005 (3)	0.005 (3)	−0.025 (3)
C30	0.146 (5)	0.122 (4)	0.091 (3)	0.018 (4)	0.002 (4)	0.027 (3)

Geometric parameters (Å, º)

C18—H18	0.9800	C15—H15A	0.9700
C18—C13	1.530 (5)	C15—H15B	0.9700
C18—C19	1.566 (5)	C15—C14	1.549 (5)
C18—C17	1.539 (5)	C19—H19	0.9800
O2—C3	1.472 (4)	C19—C20	1.549 (6)

O2—C31	1.320 (5)	C19—C29	1.510 (5)
C9—H9	0.9800	C14—C27	1.558 (5)
C9—C10	1.571 (5)	C17—C22	1.541 (6)
C9—C11	1.511 (5)	C17—C28	1.539 (6)
C9—C8	1.558 (4)	O3—C23	1.195 (5)
C5—H5	0.9800	C27—H27A	0.9600
C5—C10	1.547 (5)	C27—H27B	0.9600
C5—C6	1.534 (5)	C27—H27C	0.9600
C5—C4	1.555 (5)	O1—C31	1.201 (5)
C13—C12	1.331 (5)	C26—H26A	0.9600
C13—C14	1.518 (5)	C26—H26B	0.9600
C10—C1	1.557 (4)	C26—H26C	0.9600
C10—C25	1.544 (5)	C24—H24A	0.9600
C11—C12	1.474 (5)	C24—H24B	0.9600
C11—O5	1.230 (4)	C24—H24C	0.9600
C7—H7A	0.9700	C25—H25A	0.9600
C7—H7B	0.9700	C25—H25B	0.9600
C7—C6	1.507 (5)	C25—H25C	0.9600
C7—C8	1.546 (5)	C20—H20	0.9800
C3—H3	0.9800	C20—C21	1.516 (7)
C3—C4	1.537 (5)	C20—C30	1.508 (6)
C3—C2	1.520 (6)	C22—H22A	0.9700
C6—H6A	0.9700	C22—H22B	0.9700
C6—H6B	0.9700	C22—C21	1.499 (7)
C12—H12	0.9300	C31—C32	1.473 (6)
C4—C23	1.546 (6)	C32—H32A	0.9600
C4—C24	1.543 (5)	C32—H32B	0.9600
O4—H4	0.8200	C32—H32C	0.9600
O4—C23	1.328 (5)	C29—H29A	0.9600
C1—H1A	0.9700	C29—H29B	0.9600
C1—H1B	0.9700	C29—H29C	0.9600
C1—C2	1.521 (5)	C21—H21A	0.9700
C16—H16A	0.9700	C21—H21B	0.9700
C16—H16B	0.9700	C28—H28A	0.9600
C16—C15	1.538 (5)	C28—H28B	0.9600
C16—C17	1.539 (6)	C28—H28C	0.9600
C8—C14	1.594 (5)	C30—H30A	0.9600
C8—C26	1.559 (5)	C30—H30B	0.9600
C2—H2A	0.9700	C30—H30C	0.9600
C2—H2B	0.9700		

C13—C18—H18	106.0	C20—C19—C18	112.3 (3)
C13—C18—C19	112.4 (3)	C20—C19—H19	107.5
C13—C18—C17	111.2 (3)	C29—C19—C18	111.6 (3)
C19—C18—H18	106.0	C29—C19—H19	107.5
C17—C18—H18	106.0	C29—C19—C20	110.2 (3)
C17—C18—C19	114.3 (3)	C13—C14—C8	109.5 (3)
C31—O2—C3	118.1 (3)	C13—C14—C15	112.8 (3)

C10—C9—H9	104.1	C13—C14—C27	106.6 (3)
C11—C9—H9	104.1	C15—C14—C8	109.6 (3)
C11—C9—C10	116.8 (3)	C15—C14—C27	106.1 (3)
C11—C9—C8	107.6 (3)	C27—C14—C8	112.2 (3)
C8—C9—H9	104.1	C18—C17—C22	110.0 (3)
C8—C9—C10	118.2 (3)	C16—C17—C18	108.3 (3)
C10—C5—H5	104.4	C16—C17—C22	109.5 (4)
C10—C5—C4	115.5 (3)	C28—C17—C18	109.4 (4)
C6—C5—H5	104.4	C28—C17—C16	110.1 (4)
C6—C5—C10	111.1 (3)	C28—C17—C22	109.5 (4)
C6—C5—C4	115.4 (3)	C14—C27—H27A	109.5
C4—C5—H5	104.4	C14—C27—H27B	109.5
C12—C13—C18	120.3 (3)	C14—C27—H27C	109.5
C12—C13—C14	119.7 (3)	H27A—C27—H27B	109.5
C14—C13—C18	119.9 (3)	H27A—C27—H27C	109.5
C5—C10—C9	108.0 (3)	H27B—C27—H27C	109.5
C5—C10—C1	107.7 (3)	O4—C23—C4	111.3 (4)
C1—C10—C9	107.2 (3)	O3—C23—C4	124.7 (4)
C25—C10—C9	112.3 (3)	O3—C23—O4	123.9 (4)
C25—C10—C5	112.6 (3)	C8—C26—H26A	109.5
C25—C10—C1	108.7 (3)	C8—C26—H26B	109.5
C12—C11—C9	117.4 (3)	C8—C26—H26C	109.5
O5—C11—C9	124.0 (4)	H26A—C26—H26B	109.5
O5—C11—C12	118.6 (4)	H26A—C26—H26C	109.5
H7A—C7—H7B	107.6	H26B—C26—H26C	109.5
C6—C7—H7A	108.7	C4—C24—H24A	109.5
C6—C7—H7B	108.7	C4—C24—H24B	109.5
C6—C7—C8	114.1 (3)	C4—C24—H24C	109.5
C8—C7—H7A	108.7	H24A—C24—H24B	109.5
C8—C7—H7B	108.7	H24A—C24—H24C	109.5
O2—C3—H3	109.9	H24B—C24—H24C	109.5
O2—C3—C4	105.2 (3)	C10—C25—H25A	109.5
O2—C3—C2	107.8 (3)	C10—C25—H25B	109.5
C4—C3—H3	109.9	C10—C25—H25C	109.5
C2—C3—H3	109.9	H25A—C25—H25B	109.5
C2—C3—C4	114.0 (3)	H25A—C25—H25C	109.5
C5—C6—H6A	109.5	H25B—C25—H25C	109.5
C5—C6—H6B	109.5	C19—C20—H20	107.7
C7—C6—C5	110.6 (3)	C21—C20—C19	110.3 (4)
C7—C6—H6A	109.5	C21—C20—H20	107.7
C7—C6—H6B	109.5	C30—C20—C19	112.3 (4)
H6A—C6—H6B	108.1	C30—C20—H20	107.7
C13—C12—C11	124.9 (3)	C30—C20—C21	111.0 (4)
C13—C12—H12	117.6	C17—C22—H22A	108.4
C11—C12—H12	117.6	C17—C22—H22B	108.4
C3—C4—C5	110.1 (3)	H22A—C22—H22B	107.5
C3—C4—C23	106.5 (3)	C21—C22—C17	115.5 (4)
C3—C4—C24	108.5 (3)	C21—C22—H22A	108.4

C23—C4—C5	115.6 (3)	C21—C22—H22B	108.4
C24—C4—C5	111.1 (3)	O2—C31—C32	112.7 (4)
C24—C4—C23	104.7 (3)	O1—C31—O2	122.0 (4)
C23—O4—H4	109.5	O1—C31—C32	125.3 (4)
C10—C1—H1A	109.1	C31—C32—H32A	109.5
C10—C1—H1B	109.1	C31—C32—H32B	109.5
H1A—C1—H1B	107.9	C31—C32—H32C	109.5
C2—C1—C10	112.4 (3)	H32A—C32—H32B	109.5
C2—C1—H1A	109.1	H32A—C32—H32C	109.5
C2—C1—H1B	109.1	H32B—C32—H32C	109.5
H16A—C16—H16B	107.8	C19—C29—H29A	109.5
C15—C16—H16A	109.0	C19—C29—H29B	109.5
C15—C16—H16B	109.0	C19—C29—H29C	109.5
C15—C16—C17	112.8 (4)	H29A—C29—H29B	109.5
C17—C16—H16A	109.0	H29A—C29—H29C	109.5
C17—C16—H16B	109.0	H29B—C29—H29C	109.5
C9—C8—C14	107.6 (2)	C20—C21—H21A	109.2
C9—C8—C26	109.4 (3)	C20—C21—H21B	109.2
C7—C8—C9	110.5 (3)	C22—C21—C20	112.1 (4)
C7—C8—C14	110.6 (3)	C22—C21—H21A	109.2
C7—C8—C26	107.3 (3)	C22—C21—H21B	109.2
C26—C8—C14	111.6 (3)	H21A—C21—H21B	107.9
C3—C2—C1	113.3 (3)	C17—C28—H28A	109.5
C3—C2—H2A	108.9	C17—C28—H28B	109.5
C3—C2—H2B	108.9	C17—C28—H28C	109.5
C1—C2—H2A	108.9	H28A—C28—H28B	109.5
C1—C2—H2B	108.9	H28A—C28—H28C	109.5
H2A—C2—H2B	107.7	H28B—C28—H28C	109.5
C16—C15—H15A	108.8	C20—C30—H30A	109.5
C16—C15—H15B	108.8	C20—C30—H30B	109.5
C16—C15—C14	113.7 (3)	C20—C30—H30C	109.5
H15A—C15—H15B	107.7	H30A—C30—H30B	109.5
C14—C15—H15A	108.8	H30A—C30—H30C	109.5
C14—C15—H15B	108.8	H30B—C30—H30C	109.5
C18—C19—H19	107.5		

C18—C13—C12—C11	172.7 (3)	C6—C7—C8—C9	−46.1 (4)
C18—C13—C14—C8	157.9 (3)	C6—C7—C8—C14	−165.0 (3)
C18—C13—C14—C15	35.6 (4)	C6—C7—C8—C26	73.1 (4)
C18—C13—C14—C27	−80.4 (4)	C12—C13—C14—C8	−25.8 (4)
C18—C19—C20—C21	52.9 (5)	C12—C13—C14—C15	−148.1 (3)
C18—C19—C20—C30	177.2 (4)	C12—C13—C14—C27	95.9 (4)
C18—C17—C22—C21	−49.9 (6)	C4—C5—C10—C9	−170.3 (3)
O2—C3—C4—C5	70.1 (4)	C4—C5—C10—C1	−54.8 (4)
O2—C3—C4—C23	−163.9 (3)	C4—C5—C10—C25	65.0 (4)
O2—C3—C4—C24	−51.7 (4)	C4—C5—C6—C7	162.7 (3)
O2—C3—C2—C1	−65.0 (4)	C4—C3—C2—C1	51.4 (4)
C9—C10—C1—C2	171.1 (3)	C16—C15—C14—C13	−38.0 (5)

C9—C11—C12—C13	−1.0 (5)	C16—C15—C14—C8	−160.3 (3)
C9—C8—C14—C13	58.6 (3)	C16—C15—C14—C27	78.4 (4)
C9—C8—C14—C15	−177.2 (3)	C16—C17—C22—C21	69.0 (5)
C9—C8—C14—C27	−59.6 (3)	O5—C11—C12—C13	−179.0 (3)
C5—C10—C1—C2	55.1 (4)	C8—C9—C10—C5	−47.2 (4)
C5—C4—C23—O4	−55.8 (5)	C8—C9—C10—C1	−163.0 (3)
C5—C4—C23—O3	127.1 (5)	C8—C9—C10—C25	77.6 (4)
C13—C18—C19—C20	−177.8 (3)	C8—C9—C11—C12	34.8 (4)
C13—C18—C19—C29	57.9 (4)	C8—C9—C11—O5	−147.3 (3)
C13—C18—C17—C16	55.1 (4)	C8—C7—C6—C5	58.0 (4)
C13—C18—C17—C22	174.8 (4)	C2—C3—C4—C5	−47.8 (4)
C13—C18—C17—C28	−64.9 (4)	C2—C3—C4—C23	78.3 (4)
C10—C9—C11—C12	170.5 (3)	C2—C3—C4—C24	−169.6 (3)
C10—C9—C11—O5	−11.6 (5)	C15—C16—C17—C18	−61.3 (5)
C10—C9—C8—C7	42.1 (4)	C15—C16—C17—C22	178.7 (3)
C10—C9—C8—C14	162.9 (3)	C15—C16—C17—C28	58.3 (5)
C10—C9—C8—C26	−75.8 (4)	C19—C18—C13—C12	−91.8 (4)
C10—C5—C6—C7	−63.3 (4)	C19—C18—C13—C14	84.5 (4)
C10—C5—C4—C3	51.6 (4)	C19—C18—C17—C16	−73.6 (4)
C10—C5—C4—C23	−69.1 (4)	C19—C18—C17—C22	46.1 (5)
C10—C5—C4—C24	171.8 (3)	C19—C18—C17—C28	166.4 (4)
C10—C1—C2—C3	−55.2 (4)	C19—C20—C21—C22	−55.9 (5)
C11—C9—C10—C5	−178.2 (3)	C14—C13—C12—C11	−3.6 (5)
C11—C9—C10—C1	66.0 (4)	C17—C18—C13—C12	138.5 (4)
C11—C9—C10—C25	−53.4 (4)	C17—C18—C13—C14	−45.2 (4)
C11—C9—C8—C7	177.0 (3)	C17—C18—C19—C20	−49.7 (5)
C11—C9—C8—C14	−62.2 (3)	C17—C18—C19—C29	−174.1 (4)
C11—C9—C8—C26	59.2 (4)	C17—C16—C15—C14	53.2 (5)
C7—C8—C14—C13	179.3 (3)	C17—C22—C21—C20	56.2 (6)
C7—C8—C14—C15	−56.4 (4)	C26—C8—C14—C13	−61.4 (3)
C7—C8—C14—C27	61.1 (3)	C26—C8—C14—C15	62.8 (4)
C3—O2—C31—O1	6.8 (6)	C26—C8—C14—C27	−179.6 (3)
C3—O2—C31—C32	−174.7 (3)	C24—C4—C23—O4	66.8 (4)
C3—C4—C23—O4	−178.4 (4)	C24—C4—C23—O3	−110.4 (5)
C3—C4—C23—O3	4.4 (6)	C25—C10—C1—C2	−67.2 (4)
C6—C5—C10—C9	55.8 (3)	C31—O2—C3—C4	149.8 (3)
C6—C5—C10—C1	171.3 (3)	C31—O2—C3—C2	−88.2 (4)
C6—C5—C10—C25	−68.9 (4)	C29—C19—C20—C21	178.0 (4)
C6—C5—C4—C3	−176.5 (3)	C29—C19—C20—C30	−57.7 (5)
C6—C5—C4—C23	62.8 (4)	C28—C17—C22—C21	−170.1 (5)
C6—C5—C4—C24	−56.3 (4)	C30—C20—C21—C22	179.0 (4)

Hydrogen-bond geometry (Å, º)

D—H···*A*	*D*—H	H···*A*	*D*···*A*	*D*—H···*A*
O4—H4···O1^{i}	0.82	1.91	2.695 (4)	161
C1—H1*A*···O5	0.97	2.39	3.023 (5)	122
C25—H25*C*···O5	0.96	2.38	3.058 (5)	127

C30—H30*B*···O1^{ii}	0.96	2.60	3.468 (6)	151
C32—H32*C*···O3^{iii}	0.96	2.52	3.445 (6)	162

Symmetry codes: (i) −*x*+3/2, *y*−1/2, −*z*+3; (ii) *x*, *y*, *z*−1; (iii) *x*−1/2, −*y*+1/2, −*z*+3.